AIChE

# Optimization of Two-Dimensional Flows with Homogeneous and Heterogeneously Catalyzed Gas-Phase Reactions

**H. D. Minh**
Institute for Chemical Technology and Polymer Chemistry, University of Karlsruhe, 76131 Karlsruhe, Germany, and
Interdisciplinary Center for Scientific Computing, University of Heidelberg, 69120 Heidelberg, Germany

**H. G. Bock**
Interdisciplinary Center for Scientific Computing, University of Heidelberg, 69120 Heidelberg, Germany

**S. Tischer and O. Deutschmann**
Institute for Chemical Technology and Polymer Chemistry, University of Karlsruhe, 76131 Karlsruhe, Germany

*DOI 10.1002/aic.11563*
*Published online July 11, 2008 in Wiley InterScience (www.interscience.wiley.com).*

*Chemically reacting gaseous flows in catalytic monoliths are numerically investigated to mathematically optimize product yields by the variation of operating conditions and catalyst loading. The fluid dynamics of the single monolith channel is modeled by the two-dimensional boundary layer equations (BLEs), a system of parabolic partial differential equations (PDEs) with highly nonlinear boundary conditions arising from the coupling of surface reactions with the reactive flow field inside the channel. The surface and gas-phase chemical reactions are described by large elementary-step reaction mechanisms. An optimal control problem is formulated with the wall temperature, the catalytic active surface area, and the inlet gas composition and flow parameters as control variables. The newly developed approach and numerical code are applied for the optimization of the oxidative dehydrogenation of ethane to ethylene over platinum at high temperatures and short contact times. The ethylene yield can be significantly increased by choosing the optimal operating conditions. Furthermore, the analysis of the behavior of the reactor at optimized conditions leads to a better understanding of the interaction of physics and chemistry in the catalytic monolith.* © 2008 American Institute of Chemical Engineers *AIChE J,* 54: 2432–2440, 2008
*Keywords: computer simulations, optimization, ethane catalysis, reactive flows*

## Introduction

Heterogeneously catalyzed gas-phase reactions are part of the majority of industrial chemical processes. At high temperatures, the catalytic reactions on the solid surfaces often interact with homogeneous reactions in the gas-phase. To provide large surface areas, monolithic reactors are frequently used for heterogeneously catalyzed processes. Applications of catalytic monoliths range from small lab-scale reactors to large-scale facilities, e.g., for automotive exhaust-gas after-treatment, catalytic combustion, conversion of natural gas into synthesis gas and, subsequently, into higher

Correspondence concerning this article should be addressed to H. D. Minh at hoang.minh@kit.edu (or) O. Deutschmann at olaf.deutschmann@kit.edu

hydrocarbons, and reforming of diesel and gasoline to produce hydrogen for fuel cell-based power units.

The monoliths can be either foams with random paths or honeycomb structures consisting of numerous parallel channels. For a numerical model of the monolith, the different scales of the physical and chemical processes have to be considered. Usually, due to high space velocities, the residence time of the fluid phase inside the reactor is small when compared with the response time of the solid phase. In this case, the reacting flow in the single channel and the heat balance of the monolith can be decoupled, and the thermal behavior as well as the fluid dynamics in the individual channels can be considered simultaneously.[1] However, in this article, we only focus on the numerical simulation of the fluid phase and chemistry in a single channel of the structured monolith.

The complex interaction between molecular transport and chemical reactions has significant influence on the shape of the species profiles in such honeycomb channels of a hydraulic diameter of ~0.2–2.0 mm. The residence time of the gases inside the monolith is typically on the order of milliseconds. The diffusive transport across the channel and inside the porous catalytic layer, called washcoat, also occurs on time scales of milliseconds. The chemical reactions cover a much wider range of time scales, from nanoseconds to seconds. Since all these processes have to be considered simultaneously, the mathematical model results in a stiff system of differential equations. For mathematical optimization of the system, first of all, an efficient algorithm is needed for a fast numerical solution of equations modeling transport and chemistry in the channel.

The newly developed optimization approach is in particular suitable for better engineering of monolithic reactors with strong interaction between chemical reactions on the catalytic surface and in the gas-phase, and mass and heat transport. As an example of such a system, the catalytic oxy-dehydrogenation of ethane to ethylene in a platinum-coated catalyst is chosen. For the optimization of catalytic reactors, the objectives usually are the maximization of the yield of a product or the conversion of a pollutant, or the minimization of the energy demand or catalyst loading. In our example, the yield of the product, ethylene, should be maximized depending on inlet (temperature, species composition, mass flow) and reactor operating conditions (wall temperature and catalyst loading along the channel).

After homogeneous,[2] reactive systems and one-dimensional stagnation-flows on catalytic plates were optimized,[3,4] in this article, the optimization of two-dimensional reactive flow in a single channel of catalytic monoliths is studied. The chemical surface and gas-phase reactions are described by detailed models based on elementary-step reaction mechanisms, which were described and evaluated by comparison with experimental data in literature before.[5] Here, we have used these published mechanisms without any modification, even though a decent number of experimental and theoretical studies have been performed for the system under investigation[6–11] since the mechanisms were developed, which may require an update of the mechanisms. Oxy-dehydrogenation of ethane was chosen as an example, because it represents one of the most complex systems, for which detailed reaction mechanisms are available.[5] Thus, by choosing this complex reactive system, we demonstrate the robustness of the presented method.

## Mathematical Model

### *Fluid dynamics: boundary-layer equations*

Figure 1 illustrates the physical and chemical processes typical for a catalytic monolith and the model assumption. The fluid dynamics is modeled on the scale of a single channel. Catalytic reactors with homogeneous and heterogeneous reactions are typically characterized by a complex interaction of physical transport processes and chemical reactions on a very short time scale. Therefore, it is critical for a time-efficient simulation of the single-channel problem to choose a model that includes the necessary processes, but that also allows for a simplification of the underlying mathematical equations. Instead of solving the full Navier-Stokes equations, our model is based on two simplifying assumptions:

(1) Even though the support of the monolith often defines a square or even hexagonal structure of the channel cross section, the corners of the channel become rounded after adding a washcoat that contains the catalytic active material. This observation and the fact that the excess washcoat in the corners does not significantly contribute to the chemical reaction, allows us to approximate the channel by an axis-symmetric cylinder. (2) The elliptical structure of the steady-state Navier-Stokes equations is reduced to a parabolic one by applying the boundary-layer approximation. In the channel, the convection is mainly directed parallel to the walls as in a boundary layer of any flow around an arbitrary solid object. As a consequence, the transport in axial direction is mainly convective; the diffusive transport terms can be neglected in this direction, in particular at high Peclet numbers. In radial direction, the diffusive transport is dominating, which is expressed by a vanishing pressure gradient in that direction. It has been shown previously that the boundary-layer approximation is a suitable model for the description of the flow in a monolith channel for a wide range of Reynolds numbers, especially for conditions as in short contact-time reactors or exhaust gas after-treatment devices.[12,13] Therefore, in this article, the boundary layer equations,[13–16] which are a system of parabolic partial differential equations with nonlinear boundary conditions, are used as model for the fluid dynamics. For more details of the equations and their coupling to multiphase complex reaction networks, we refer to those references and the user manual of the code applied.[17]

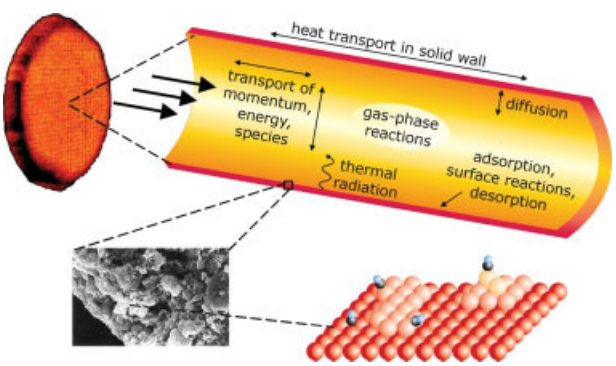


**Figure 1. Processes occurring in a catalytic monolith operated at high temperature.**

[Color figure can be viewed in the online issue, which is available at www.interscience.wiley.com.]

Detailed models are used for the chemistry in the gas-phase and on the surface. The forward rate coefficients $k_{fi}$ of the gas-phase reaction $i$ are calculated by using an Arrhenius type expression:

$$k_{fi} = A_i T^{\beta i} \exp\left(-\frac{E_{ai}}{RT}\right), \tag{1}$$

where $A_i$ is the pre-exponential factor, $\beta_i$ the temperature exponent, and $E_{ai}$ is the activation energy of the $i$th reaction, $R$ is the universal gas constant being 8.314 J/(mol K), and $T$ is the gas temperature. The reverse rate coefficients, $k_{ri}$, are determined from thermodynamics. The forward rate coefficient $k_{fi}$ of surface reactions $i$ is calculated by a modified Arrhenius expression

$$k_{fi} = A_i T^{\beta i} \exp\left(-\frac{E_{ai}}{RT}\right) \prod_{k=1}^{K_s} \theta_k^{\mu_{ki}} \exp\left(\frac{\varepsilon_{ki}\theta_k}{RT}\right), \tag{2}$$

where $\mu_{ki}$ and $\varepsilon_{ki}$ are parameters describing an additional dependence of the rate on the surface coverage. $\mu_{ki}$ and $\varepsilon_{ki}$ are often set to zero due to lack of information on those dependencies. $\theta_k$ is the surface coverage of the $k$th surface (adsorbed) species, which must satisfy the following conditions:

$$0 \le \theta_k \le 1 (k = 1, \ldots, N_s), \quad \sum_{k=1}^{N_s} \theta_k = 1 \tag{3}$$

where $N_s$ is the number of surface species.

### Initial and boundary conditions

At the catalytic surface, the gaseous species mass flux produced by heterogeneous chemical reactions and the mass flux of that species in the gas phase at the gas-surface boundary must be balanced, i.e.,

$$F_{cat/geo} \dot{s}_k W_k = -J_{kr} \quad (k = 1, \ldots, N_g) \tag{4}$$

where

$$\dot{s}_k = \sum_{i=1}^{k_s} \nu_{ik} k_{fk} \prod_{j=1}^{N_g+N_s} c_j^{\nu'_{jk}},$$

is the creation or depletion rate of the $k$th species due to the adsorption, desorption, and chemical reactions on the surface, $W_k$ is its molar mass of the $k$th species. $J_{kr}$ represent the radial components of the diffusive flux vector of species $k$ pointing from the center to the wall. The factor $F_{cat/geo}$ describes the ratio of catalytic to geometric surface areas, which corresponds to the amount of catalyst available for surface reactions; $F_{cat/geo} = 1$ would mean that the inner channel wall is completely coated with a monolayer catalytic film. The use of washcoats can easily lead to values for $F_{cat/geo}$ on the order of $10^2$. This parameter will play an important role in the optimal control problem.

In this study, potential mass transfer limitation of the conversion due to finite diffusion in the pores of the washcoat is neglected. Within the software[17] used, this mass transfer effect can be introduced by the addition of an "on-the-fly" computed effectiveness factor into the boundary conditions (4) or by the very time-consuming solution of reaction-diffusion equations for the washcoat layer coupled with the 2D flow field model.

Since we calculate the steady-state of the system, in this study, all adsorbed species (surface species) will obey the condition,

$$\dot{s}_k = 0 \quad (k = N_g + 1, \ldots, N_g + N_s) \tag{5}$$

This condition also remains valid for most, not too fast, transient processes[1] but breaks down for very fast transients such as catalytic ignition, which proceeds within $10^{-6}$ s.[18]

### Application example: oxidative dehydrogenation of ethane

A promising route for the production of ethylene ($C_2H_4$) are so-called short-contact time reactors, where ethane ($C_2H_6$) is dehydrogenated by partial oxidation.[19] Here, a mixture of ethane, oxygen, nitrogen, and possibly hydrogen is fed into a catalytically coated monolith. The residence time of the gases is only ~5 ms at temperatures between 1150 and 1300 K. The advantage of oxygen addition in a dehydrogenation process is that the catalytic oxidation of some of the ethane provides a sufficient amount of heat for the endothermic dehydrogenation, which permits autothermal operation of the reactor at those high temperatures. Bodke et al.[20] reported high ethylene selectivity of up to 70% at complete oxygen and high ethane conversion; hence, the yield of the reactor can compete with the conventional steam cracking of ethane. Later, Beretta et al.[6,21] have conducted similar experiments confirming the results and supporting the hypothesis that most of the ethylene is produced in the gas-phase.

Zerkle et al.[5] have studied the system numerically. Their gas-phase mechanism consists of 25 reactive species (mainly $C_1$ and $C_2$ species) involved in 131 reversible reactions and one irreversible reaction. In addition, a surface reaction mechanism was established for the conversion over platinum consisting of another 82 elementary-step like reactions involving another 19 surface species. This mechanism was later also used to study on-line catalyst addition effects.[22]

Our example for the optimal control problem is based on the case studied by Zerkle et al.[5] The monolith itself has a diameter of 18 mm and a length of 10 mm. The individual channels have a diameter of 0.5 mm. The monolith is fed with ethane/oxygen/nitrogen mixture of varying C/O ratio at 5 standard liters per minute.

### Formulation of an optimal control problem

In a chemical reactor, the initial and boundary conditions can be used to optimize the performance of the reactor, i.e., maximize the conversion, the selectivity, or the yield of certain product species. In particular, at the inlet of the catalytic monolith, the chemical composition, the velocity, and the temperature can be controlled to optimize the product composition. Furthermore, it may be possible to control the temperature profile $T_{wall}(z)$ at the channel wall and vary the catalyst loading along the channel, i.e., $F_{cat/geo}(z)$; $z$ is the axial spatial coordinate. Moreover, the length of the catalytic monolith, $z_{max}$, can be optimized as well.

In general, this optimization problem can be stated as

$$\min_{w,q} \Phi(w) \tag{6}$$

Subject to PDE Model Equation $(w, q)$ (7)

Initial and Boundary Condition $(w, q)$ (8)

State and Control Constraints $(w, q)$ (9)

where $w$ and $q$ are state and control variables, respectively. The partial differential equations (PDE) equations describe the fluid dynamics and the gas-phase chemistry. The initial and boundary conditions are given by Eqs. 4 and 5.

### *Objective function*

The objective function to be maximized is the mass fraction of ethylene at the outlet of the channel:

$$\Phi(w) = Y_{C_2H_4}$$

at outlet.

### *Controls*

The controls considered here are the inlet gas composition, temperature, velocity, and pressure, which are independent of the axial coordinate $z$, and the wall temperature $T_{\text{wall}}(z)$ and/or the catalyst loading, expressed by $F_{\text{cat/geo}}(z)$, which are functions of the axial coordinate $z$.

### *Constraints*

For practical reasons, there are often equality and inequality constraints on the control and state variables, such as upper and lower bounds for the wall temperature and $F_{\text{cat/geo}}$, or the fact that the sum of all mass fractions must be unity.

## Numerical Method

### *DAE-constrained optimization*

We choose the approach of semi-discretization of the PDE system in the streamline direction by the method of lines,[23] which leads to a system of structured, stiff differential algebraic equations (DAE). This transforms the optimal control problem in a PDE (6–9) to an optimal control problem in a DAE, which can be written as

$$\min_{x,q} \Phi(x, q) \tag{10}$$

Subject to The resulting DAE (11)

State and control constraints $(x, q)$ (12)

### *Direct method*

To transform the optimal control problem (10–12) to a finite dimensional optimization problem, we apply the direct approach; this means we parameterize the control functions by a finite number of degrees of freedom.

### *Parameterization of the control functions*

The profiles at the wall $T_{\text{wall}}(z)$ and $F_{\text{cat/geo}}(z)$ are treated as control function in the optimal control problem. Control functions are discretized on an appropriate user-defined grid using a suitable finite functional basis. Usually, the controls are approximated by piecewise continuous functions, e.g., piecewise constant or piecewise linear, but also other schemes are applicable. The coefficients in these schemes will be control parameters replacing the control functions. By this way, the control function in infinite-dimensional space is approximated by its piecewise representation in a finite-dimensional space. If the piecewise linear approximation is applied, then

$$T_{\text{wall}}(z) = T_{\text{wall}}(z_j) + \left(T_{\text{wall}}(z_{j+1}) - T_{\text{wall}}(z_j)\right)\frac{z - z_j}{z_{j+1} - z_j}$$
$$\text{for } z_j \le z \le z_{j+1}.$$

Note that in this case, the bounds on the controls are transformed to bounds on the parameterization coefficients.

### *Solution of the DAE system*

For the given initial values and control parameters, we solve the DAE initial value problem. The obtained solution of the DAE system is used for the evaluation of the objective function and the constraints. The DAE system is usually stiff, because it is derived from the discretization of a PDE and due to chemical reaction kinetics. The DAE is of index 1. Therefore, we choose an implicit integration method, based on backward differentiation formulas (BDF) for the solution of the initial value problems. For the practical computation, based on the code DAESOL,[24,25] we develop a new code that allows us to solve this problem. Features of this code are variable step size and variable order controlled by error estimation, modified Newton's method for the solution of the implicit nonlinear problems, a monitor strategy to control the computation and decomposition of the Jacobian, and Internal Numerical Differentiation for the computation of derivatives of the solution w.r.t. initial values and parameters.

In our problems, the linear systems arising in Newton's method are very ill-conditioned. We have developed an appropriate scaling. The variables are scaled with the same weighting vector that is used in the BDF error estimation, and then we perform row equilibration. The scaling factors are chosen to be integer powers of the machine base to avoid scaling round-off errors. Using this technique, the condition number of the linear system is reduced from more than $10^{18}$ to around $10^7$.

The BDF method needs derivatives of the DAE model functions. Here, we exploit the band structure. Instead of computation of the full Jacobian, we apply a compression technique which only requires few directional derivatives. We use Automatic Differentiation (implemented in the tool ADIFOR[26]) that allows us to compute derivatives with accuracy up to machine precision. This is crucial for a fast performance of the overall solution method.

To solve the DAE, we compute consistent initial values for the algebraic variables. During the integration, the consistency is preserved because the algebraic constraints and the equation from the implicit integration scheme are solved simultaneously.

### *Computation of consistent initial values of the DAE*

To integrate the DAE system, a set of consistent initial values is needed. Some of them are explicitly given, as stated in previous sections. However, the mass fractions $Y_k (k = 1,\ldots, N_g)$ at the catalytic wall $\psi = \psi_N$ and the surface coverage fractions $\theta_k (k = 1,\ldots, N_s)$ are only implicitly determined by the nonlinear equations at the boundary. These equations are highly nonlinear due to the Arrhenius kinetics. The solution is the steady state of a dynamic system, which is an asymptotic limit of the corresponding transient system. We only know initial values of the transient system, which can change very drastically until the system reaches a steady state. It is very difficult to find values that are sufficiently close to the consistent values to have convergence of a Newton-type method. For this problem, techniques of globalization of the convergence often fail because nonsingularity of the Jacobian cannot be guaranteed. Therefore, we use a time-stepping method for solving the corresponding transient system to find an initial guess close to the solution and then apply Newton's method to converge to the solution.

With the variables $\left(Y_{1N,\ldots,} Y_{N_gN}, \theta_1, \ldots, \theta_{N_s}\right) \in \Re^{N_g+N_s}$, the nonlinear equation system for the boundary is

$$F_{\text{cat/geo}} \dot{s}_k W_k + J_{kr}|_{\Psi=\Psi_N} = 0 \quad (k = 1, \ldots, N_g), \tag{13}$$

$$\dot{s}_k = 0 \quad (k = N_g + 1, \ldots, N_g + N_s). \tag{14}$$

The left-hand sides of Eq. 14, $\dot{s}_k$, are the rates of creation/depletion of the surface species coverage multiplied by the site density, $\Gamma$:

$$\frac{\partial \theta_k}{\partial t} = \frac{\dot{s}_k}{\Gamma} \quad (k = N_g + 1, \ldots, N_g + N_s) \tag{15}$$

Similarly, the left-hand side of Eq. 13 can be considered as the mass rate of creation/depletion of the $k$th gas species by surface reactions and molecular diffusion in the gas-phase multiplied by some length $dr$, i.e.,

$$\rho dr \frac{\partial \theta_k}{\partial t} = F_{\text{cat/geo}} \dot{s}_k W_k + J_{kr}|_{\Psi=\Psi_N} \quad (k = 1, \ldots, N_g) \tag{16}$$

The differential equations (15 and 16) describe the corresponding transient state model for the nonlinear equations (13 and 14).

Starting from initial values for mass fractions and surface coverages $(Y_{1N}, \ldots, Y_{N_gN}, \theta_1, \ldots, \theta_{N_s})(t_0)$, we integrate the ordinary differential equation (ODE) (15 and 16) until it nearly reaches steady state. In our implementation, we monitor the value of the norm of the right-hand side, when it decreases below a certain value then we switch to Newton's method. From our practical experience, this method is quite stable even for ill-conditioned problems.

The system (15 and 16) describes a chemical process modeled by detailed chemistry and therefore it is very stiff. For solution, we also use the BDF method implemented in the new DAESOL. To speedup the computation, we only integrate until we are near steady state and then use Newton's method for fast convergence. Therefore, we do not need high tolerance for the ODE integration, which makes the integration procedure fast.

### *Nonlinear optimization problem*

The parameterization of the controls and the states turns the dynamic optimization problem into a finite dimensional optimization problem. It is a nonlinear constrained optimization problem (NLP), which can be written in general as follows:

$$\begin{aligned} \min_v \quad & F(v) \\ \text{Subject to} \quad & E(v) = 0 \\ & G(v) \geq 0 \end{aligned} \tag{17}$$

The time-independent control variables $q$ and the control parameters introduced by the parameterization of the control functions are the optimization variables $v$ in the NLP.

## Optimization Results

The results presented here summarize our application of the code to the optimization of partial oxidation of ethane over Pt catalysts. The chemical processes are described by 25 gas phase species, 20 surface species, 261 gas-phase reactions, and 82 surface reactions.[5] The work presented in this article is the first realization of optimization for this problem. For more details on the numerical algorithms, we refer to Refs. 17 and 27.

### *2D profiles of major species with initial settings*

We run a reference case simulation with the following initial settings: inlet mass fractions $Y_{C2H6} = 0.44$, $Y_{O2} = 0.26$, $Y_{N2} = 0.30$, inlet gas temperature $T_{gas} = 650$ K, inlet velocity $u_0 = 0.5$ m/s. The wall temperature was kept fixed at 930 K and $F_{\text{cat/geo}}(z) = 1$. Figures 2 and 3 show the two-dimensional profiles of major species and surface coverages with the these setting.

Clearly, three regions can be recognized along the catalyst. In the first ~1 mm, oxygen is consumed completely. Here, ethane is primarily oxidized to $CO_2$ and water on the Pt surface: the primarily adsorbed species on the surface is oxygen supporting total oxidation. The gradients in the concentration profiles for these species indicate that catalytic surface reactions fully dominate the oxidation. The overall reaction rate is limited by mass transfer, i.e., diffusion of oxygen and ethane to the catalytic surface. Since CO is an intermediate in total oxidation and is not strongly bound to the surface, some of the CO will desorb and lead to the CO peak at the entrance. However, since CO also has a high sticking coefficient on Pt, it will readsorb on the surface and be oxidized to $CO_2$ when more empty sites, Pt(s), are available due to decreasing oxygen coverage. Therefore, at $z = 0.5$ mm, a small region of decreased CO concentration in the gas-phase can be observed (Fig. 2). Since shortly further downstream, the oxygen concentration and coverage decline rapidly, there

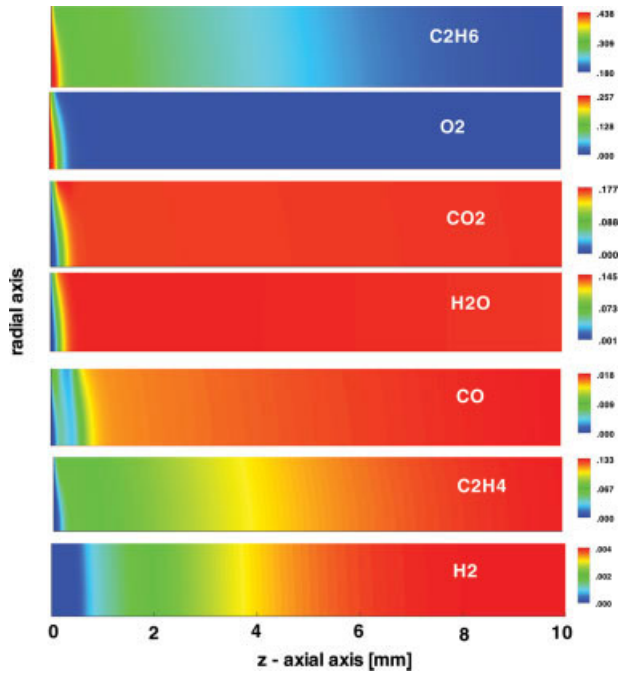


**Figure 2. Mass fraction profiles of major species with initial settings.**

The center line of the channel is at the bottom, the catalytic wall at the top of each profile; and the channel diameter is 0.5 mm.

is not enough oxygen for CO oxidation, thus, CO concentration increases again. CO also is in a small region around $z$ = 1.2 mm the species primarily adsorbed. Further downstream, all the oxygen coverage declines further and originates now from readsorbed water only. Since no oxygen is available anymore, the carbon coverage increases.

The dehydrogenation of ethane is a much slower process. After a first small region of oxygen-supported ethylene formation due to surface reactions, ethylene concentrations stay relatively constant until, further downstream, production of ethylene by pryolysis of ethane in the gas-phase becomes significant. The radial gradients in the species concentrations vanish. The process, downstream the initial oxidation section, is kinetically controlled, which is caused by the increasing rate of gas-phase reactions or by surface reactions with small

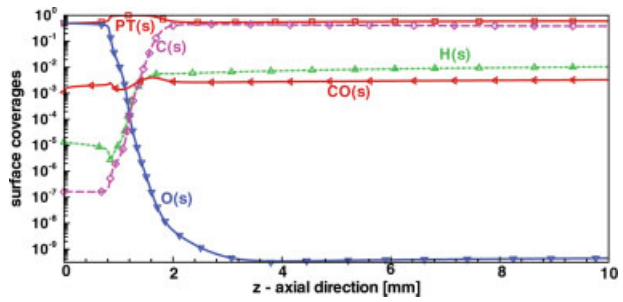


**Figure 3. Surface coverages of major adsorbed species with initial settings.**

[Color figure can be viewed in the online issue, which is available at www.interscience.wiley.com.]

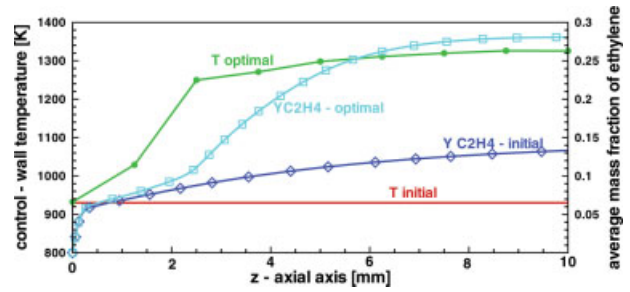


**Figure 4. Initial and optimal profiles of temperature and ethylene mass fraction.**

[Color figure can be viewed in the online issue, which is available at www.interscience.wiley.com.]

rates, after all oxygen is consumed. The continuous formation of CO is due to the water–gas-shift reaction.

### *Optimization of the wall temperature*

For the first optimization step, we keep the initial values at the inlet fixed: inlet mass fractions $Y_{C2H6}$ = 0.44, $Y_{O2}$ = 0.26, $Y_{N2}$ = 0.30, inlet gas temperature $T_{gas}$ = 650 K, inlet velocity $u_0$ = 0.5 m/s.

For the optimization of the wall temperature profile, a piecewise linear parameterization with eight intervals is used. The objective is to maximize the mass fraction of ethylene at the outlet. As constraint, the temperature is required to be between 600 and 1500 K.

The optimization was started with a constant temperature profile of 930 K leading to an objective value of 0.13. The optimization run took 30 min computational time on a 2.5-GHz Pentium 4 Linux PC. In the optimal solution, the objective value is 0.28 that means the ethylene yield could drastically be increased by an optimum temperature profile. Discussion of how this temperature profile is enforced is beyond the scope of this article. Figure 4 shows the temperature profile, and Figures 5 and 6 show the mass fraction of some major species with initial and optimal setting.

### *Control $F_{cat/geo}(z)$*

The ratio of catalytic active surface area to geometric surface area $F_{cat/geo}(z)$, i.e., the catalyst loading along the reac-

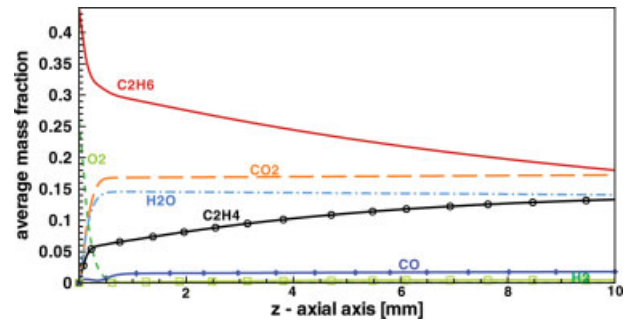


**Figure 5. Average mass fractions of major species with initial settings.**

[Color figure can be viewed in the online issue, which is available at www.interscience.wiley.com.]

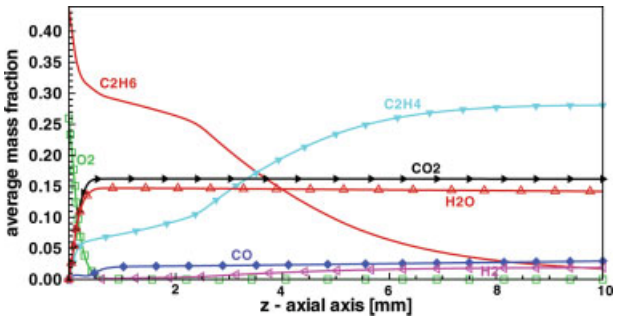


**Figure 6. Average mass fractions of major species at the optimal solution.**

[Color figure can be viewed in the online issue, which is available at www.interscience.wiley.com.]

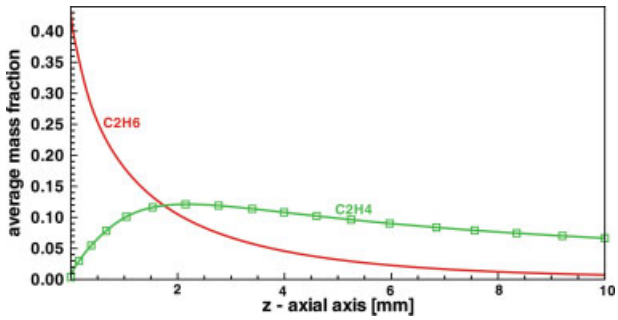


**Figure 8. Average mass fraction profiles of $C_2H_6$ and $C_2H_4$ with the initial setting.**

[Color figure can be viewed in the online issue, which is available at www.interscience.wiley.com.]

tor, is now optimized. The inlet gas temperature is $T_{gas}$ = 600 K, and the wall temperature $T_{wall}(z)$ is kept fixed at 1000 K. The objective is to maximize the mass fraction of ethylene $Y_{C2H4}$ at the outlet. As constraint, $F_{cat/geo}(z)$ is required to be between 0, i.e., no catalyst, and 100, i.e., highly loaded.

The optimization was started with a constant $F_{cat/geo}(z)$ of 20.0 leading to an objective value of 0.06. In the optimal solution, the objective value is 0.19. Figure 7 shows the standard and optimal profiles of $F_{cat/geo}(z)$ and average mass fraction profiles of ethylene. Figures 8 and 9 show the mass fraction profiles of ethane and ethylene with the standard and optimal profiles of $F_{cat/geo}(z)$.

Platinum is a very efficient catalyst for the oxidation of ethane. In the first 2 mm of the catalyst, oxygen is almost completely consumed by surface reactions (catalytic oxidation of ethane) leading to the total oxidation products $CO_2$ and $H_2O$ with some ethylene and CO as side products. Ethylene, however, can in general be produced in the gas-phase as well. However, the conversion in the gas-phase occurs only if a sufficiently large radical pool exists, which takes a certain time/distance (so-called ignition delay time) to be built-up. Furthermore, some of the ethylene formed by surface reactions adsorb on the surface as well, where in the region around $z$ = 2 mm reforming reactions mainly occur but their reaction rate is much smaller than the total oxidation rate at $z < 1$ mm, where oxygen is still available. Since the production of ethylene by gas-phase reactions reaches much higher values further downstream (most of the ethylene is produced in the gas-phase) due to the radicals available there and due to the fact that the surface is relatively inactive in the region around 2 mm, a plateau appears in that region (Figures 7 and 9) due to the competition between ethylene production in the gas-phase and (partial) oxidation on the surface, both at relatively low rates. The optimization of the catalyst loading proposes a very low loading in this region, because here the catalyst does not only oxidize ethylene but also adsorbs radicals from the gas-phase, which are needed to initiate ethylene formation in the gas-phase.

The optimization proposes relatively low catalyst loading in the very active initial catalyst section, which can be understood as follows: Within the first millimeter of the catalyst, where oxygen is available, the process is limited by mass-transfer of ethane and even more of oxygen to the surface. Here, primarily, oxidation of ethane occurs at a very high rate, the catalyst is very active. Consequently, catalyst is needed here but not at a high loading; this effect has also been observed in several experiments.

We have also implemented multivariable optimization. However according to numerical experiments, the objective function did not have significant improvement when compared with optimal objective value of a single variable optimization. The computational time for a multivariable optimization is about 50–400% increase compared to the case of

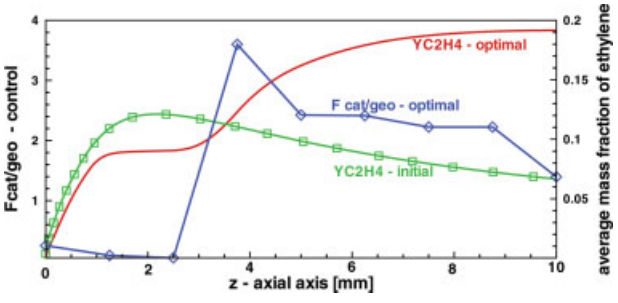


**Figure 7. $F_{cat/geo}(z)$ profile and the average mass fraction of $C_2H_4$ at the initial and at optimal solutions.**

[Color figure can be viewed in the online issue, which is available at www.interscience.wiley.com.]

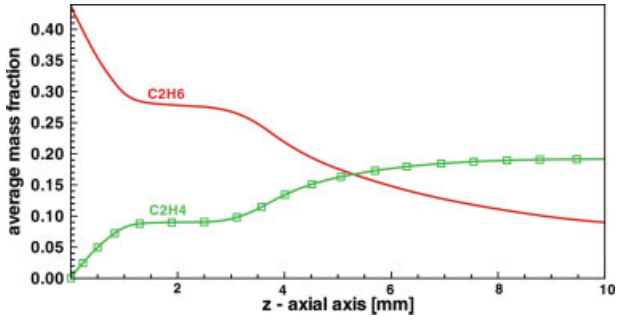


**Figure 9. Average mass fraction profiles of $C_2H_6$ and $C_2H_4$ with the optimal setting.**

[Color figure can be viewed in the online issue, which is available at www.interscience.wiley.com.]

optimization with respect to the wall temperature or catalyst loading alone, depending on the initial setting.

### *Control of the inlet gas composition*

Here, we investigate an adiabatic case. The initial inlet gas temperature was 800 K, $F_{cat/geo}(z) = 1$. The optimization was started with the initial inlet mass fractions of $Y_{C2H6} = 0.40$, $Y_{O2} = 0.30$, $Y_{N2} = 0.30$ leading to the objective value (mass fraction of ethylene at outlet) of 0.15. In the optimal setting, $Y_{C2H6} = 0.48$, $Y_{O2} = 0.22$, $Y_{N2} = 0.30$, the objective value is 0.27.

### *Control of pressure and velocity*

We have also investigated the effect of pressure and velocity; however, no significant improvement on the objective function was obtained.

## Conclusion

In this article, we presented a newly developed code for the optimization of a two-dimensional flow in a catalytic active channel. Here, the chemical reactions in the gas phase and on catalytic surfaces are modeled by detailed mechanisms consisting of elementary step-like reactions. As an example, the oxidative dehydrogenation of ethane to ethylene over Pt in a short contact time reactor was simulated. As control parameters, the influence of the wall temperature profile, the catalyst distribution, and the inlet composition on the ethylene yield were investigated. An optimal solution could be computed very time efficiently (30 min on a 2.5-GHz Pentium 4 Linux PC). Thus, for example, we were able to achieve ethylene yield that are twice as much as in our reference case.

In future, this numerical code can be applied to similar cases, for instance by applying to different reacting systems with different objectives. There is a high potential, especially in the optimization of catalyst distribution. It is a time-efficient alternative to try-and-error experimental investigations in such areas.

Since the current implementation of the optimization code is not yet applicable to consider heat conduction in the solid structure of the monolithic reactor, future work will include the extension of the underlying physical models. The simulation code of the software package used, DETCHEM$^{MONOLITH}$, already includes even transient heat balances of the solid monolithic structure coupled to single channel simulations.[28] However, the implementation of heat transfer usually requires the solution of an elliptic problem. So far, we have used the boundary layer approximation as basis for the simulation of the channel flow, which leads to a parabolic problem, that is solved very CPU time-efficiently. Therefore, new algorithmic approaches are needed.

Aside from expecting new numerical facilities of that optimization procedure, we are currently using the results of the optimization to improve reactor design. In particular, we study the proposed catalyst loadings distributed inhomogeneously in the flow direction.

## Acknowledgments

The authors thank Robert J. Kee (Colorado School of Mines), Hoang Xuan Phu (Institute of Mathematics, Vietnamese Academy of Science and Technology), and Johannes Schlöder (Heidelberg University) for many helpful discussions. The financial support from the German Science Foundation (DFG) within the Graduiertenkolleg "Complex Processes: Modeling, Simulation and Optimization", SFB 359 "Reactive Flows, Diffusion and Transport", and the project DE 659/5 is greatly acknowledged.

## Notation

$A_i$ = pre-exponential factor of the $i$th reaction
$E_{ai}$ = activation energy of the $i$th reaction
$F_{cat}/_{geo}$ = ratio of catalytic active to geometric surface areas
$J_{kr}$ = radial component of mass flux vector of the $k$th species
$N_g$ = total number of gas-phase species
$N_s$ = total number of surface species
$K_s$ = total number of surface reactions
$R$ = universal gas constant
$T$ = temperature
$W_k$ = molecular weight of the $k$th species
$Y_k$ = mass fraction of the $k$th species
$k_{fi}$ = reaction rate coefficient of the $i$th reaction
$\dot{s}_k$ = rate of production of $k$th species by surface reactions
$c_j$ = concentration of $j$th species
$u$ and $v$ = axial and radial components of the velocity vector
$z$ and $r$ = axial and radial cylindrical coordinates.
$\beta_i$ = temperature exponent of the $i$th reaction,
$\Gamma$ = surface site density
$\theta_k$ = coverage of the $k$th surface species

## Literature Cited

1. Tischer S, Deutschmann O. Recent advances in numerical modeling of catalytic monolith reactors. *Catal Today*. 2005;105:407–413.
2. Schwerin MV, Deutschmann O, Schulz V. Process optimization of reactive systems by partial reduced SQP methods. *Comput Chem Eng*. 2000;24:89–97.
3. Grosshans O. Optimal control of a reactive stagnation point flow on a catalytic plate, PhD Thesis, Mathematisch-Naturwissenschaftliche Gesamtfakultät, University of Heidelberg, Heidelberg, 2001.
4. Raja LL, Kee RJ, Serban R, Petzold LR. Computational algorithm for dynamic optimization of chemical vapor deposition processes in stagnation flow reactors. *J Electrochem Soc*. 2000;147:2718–2726.
5. Zerkle DK, Allendorf MD, Wolf M, Deutschmann O. Understanding homogeneous and heterogeneous contributions to the partial oxidation of ethane in a short contact time reactor. *J Catal*. 2000;196:18–39.
6. Beretta A, Ranzi E, Forzatti P. Production of olefins via oxidative dehydrogenation of light paraffins at short contact times. *Catal Today*. 2001;64:103–111.
7. Bodke AS, Henning D, Schmidt LD, Bharadwaj SS, Maj JJ, Siddall J. Oxidative dehydrogenation of ethane at millisecond contact times: effect of $H_2$ addition. *J Catal*. 2000;191:62–74.
8. Donsi F, Pirone R, Russo G. Oxidative dehydrogenation of ethane over a perovskite-based monolithic reactor. *J Catal*. 2002;209:51–61.
9. Donsi F, Williams KA, Schmidt LD. A multistep surface mechanism for ethane oxidative dehydrogenation on Pt-and Pt/Sn-coated moniliths. *Ind Eng Chem Res*. 2005;44:3453–3470.
10. Donsi F, Cimino S, Di Benedetto A, Pirone R, Russo G. The effect of support morphology on the reaction of oxidative dehydrogenation of ethane to ethylene at short contact times. *Catal Today*. 2000; 105:551–559.
11. Huff MC, Androulakis IP, Sinfelt JH, Reyes SC. The contribution of gas-phase reactions in the Pt-catalyzed conversion of ethane-oxygen mixtures. *J Catal*. 2000;191:46–54.
12. Koop J, Deutschmann O. Modeling and simulation of $NO_X$ abatement with storage/reduction catalysts for lean burn and diesel engines, SAE Technical Paper 2007–01-1142, SAE, 2007.
13. Raja LL, Kee RJ, Deutschmann O, Warnatz J, Schmidt LD. A critical evaluation of Navier-Stokes, boundary-layer, and plug-flow models of the flow and chemistry in a catalytic-combustion monolith. *Catal Today*. 2000;59:47–60.

14. Coltrin ME, Kee RJ, Miller JA. A mathematical model of the coupled fluid mechanics and chemical kinetics in a chemical vapor deposition reactor. *J Electrochem Soc*. 1984;131:425–434.
15. Tischer S, Correa C, Deutschmann O. Transient three-dimensional simulation of a catalytic combustion monolith using detailed models for heterogeneous and homogeneous reactions and transport phenomena. *Catal Today*. 2001;69:57–62.
16. Kee RJ, Coltrin ME, Glarborg P. *Chemically Reacting Flow: Theory and Practice*. Hoboken, NJ: Wiley, 2003.
17. Deutschmann O, Tischer S, Kleditzsch S, Janardhanan VM, Correa C, Chatterjee D, Mladenov N, Minh HD. DETCHEM Software Package, 2.1 ed. Karlsruhe, 2007. www.detchem.com.
18. Deutschmann O, Schmidt R, Behrendt F, Warnatz J. Numerical modeling of catalytic ignition. *Proc Combust Inst*. 1996;26:1747–1754.
19. Huff M, Schmidt LD. Ethylene formation by oxidative dehydrogenation of ethane over monoliths at very short contact times. *J Phys Chem*. 1993;97:11815–11822.
20. Bodke AS, Bharadwaj SS, Schmidt LD. The effect of ceramic supports on partial oxidation of hydrocarbons over noble metal coated monoliths. *J Catal*. 1998;179:139–149.
21. Beretta A, Ranzi E, Forzatti P. Oxidative dehydrogenation of light paraffins in novel short contact time reactors. Experimental and theoretical investigation. *Chem Eng Sci*. 2001;56:779–787.
22. Zerkle DK, Allendorf MD, Wolf M, Deutschmann O. Modeling of on-line catalyst addition effects in a short contact time reactor. *Proc Combust Inst*. 2000;28:1365–1372.
23. Schiesser WE. *The Numerical Method of Lines, Integration of Partial Differential Equations*. San Diego, CA: Academic Press, 1991.
24. Bauer I, Bock HG, Schlöder JP. DAESOL—a BDF-code for the numerical solution of differential algebraic equations, Technical report, SFB 359, IWR, Heidelberg University, Heidelberg, 1999.
25. Bauer I, Finocchi F, Duschl WJ, Gail H-P, Schlöder JP. Simulation of chemical reactions and dust destruction in protoplanetary accretion disks. *Astron Astrophys*. 1997;317:273–289.
26. Bischof C, Carle A, Hovland P, Khademi P, Mauer A. ADIFOR 2.0 User's Guide, Mathematics and Computer Science Division, Argonne National Laboratory, 1995.
27. Minh HD. Numerical methods for simulation and optimization of chemically reacting flows in catalytic monoliths, PhD Thesis, Faculty of Mathematics and Computer Science, University of Heidelberg, Heidelberg, December 2005.
28. Schwiedernoch R, Tischer S, Correa C, Deutschmann O. Experimental and numerical study of the transient behavior of a catalytic partial oxidation monolith. *Chem Eng Sci*. 2003;58:633–642.

*Manuscript received Aug. 21, 2007, and revision received Apr. 4, 2008.*